MOVING-WINDOW ICA DECOMPOSITION OF EEG DATA REVEALS EVENT-RELATED CHANGES IN OSCILLATORY BRAIN ACTIVITY

Scott Makeig*, Sigurd Enghoff (3,4).
Tzyy-Ping Jung (3,5,6) and Terrence J. Sejnowski (2,3,5,6)

*Naval Health Research Center, San Diego CA; (2) Howard Hughes Medical Institute; (3) Computational Neurobiology Laboratory, The Salk Institute for Biological Studies; (4) Danish Technical University; (5) Institute for Neural Computation; (6) University of California San Diego, La Jolla CA

Abstract. Decomposition of temporally overlapping sub-epochs from 3-s electroencephalographic (EEG) epochs time locked to the presentation of visual target stimuli in a selective attention task produced many more components with common scalp maps before stimulus delivery than after it. In particular, this was the case for components accounting for posterior alpha and central mu rhythms. Moving-window ICA decomposition thus appears to be a useful technique for evaluating changes in the independence of activity in different brain regions, i.e. event-related changes in brain dynamic modularity. However, common component clusters found by moving-window ICA decomposition strongly resembled those found by decomposition of the whole EEG epochs, suggesting that such whole epoch decomposition reveals stable independent components of EEG signals.

Introduction

The application of ICA or blind source separation to human brain electromagnetic data shows much promise (Makeig et al., 1996). Applied to a collection of average responses, ICA can separate the observed spatially labile activity into spatially fixed components that parsimoniously account for the responses in all the conditions (Makeig et al., 1997). Detailed examination of the activity of these components may show distinct, systematic relationships to condition differences and, moreover, to subject behavior, thereby revealing neuropsychological aspects of performance in the studied conditions (Makeig et al., 1999a, 1999b). However, the artificial temporal overlap in the underlying EEG sources induced by response averaging means that ICA may be optimally applied to averaged evoked response data only under certain conditions, including high signal to noise ratio and the availability of many contrasting response conditions.

A more general and promising procedure is to blindly decompose collections of single-trial EEG recordings from event-related response experiments into spatially fixed, temporally independent components (Makeig et al., 1996; Vigario et al., 1997; Jung et al., 1998, 1999). This procedure allows ICA to use trial-to-trial variations in relative amplitudes, latencies and phases of coherent activity in different brain networks to separate them.

One major category of independent EEG components comprise the so-called EEG artifacts generated by eye blinks, eye movements, and scalp muscle activity can be used for removing evidence of these artifact sources from event-related EEG time windows or epochs prior to averaging (Jung et al., 1999, in press). ICA can also be applied to event-related EEG epochs. The dynamics of brain networks that participate in event-related information processing can be measured over time both after and before experimental events of interest. Response averaging, which has dominated the field of event-related human brain dynamics for the last 30 years, has obscured an important question: Are spontaneous EEG dynamics related to event-related responses, and if so, how?

The limits of the usefulness of ICA, and in particular, infomax ICA, for EEG analysis will ultimately depend on the fit between the assumptions of the analysis method and the composition of EEG data. Here, we attempted to examine two assumptions of infomax: (1) that EEG sources are spatially fixed, and (2) that the effective number of independent sources is fewer than the available number of recording channels (here, 31). We introduce first a method of decomposing data by applying infomax ICA successively to sets of brief data windows defined by their relative temporal relationship to some class of experimental events, here visual stimuli to which subjects were instructed to respond with a button press.
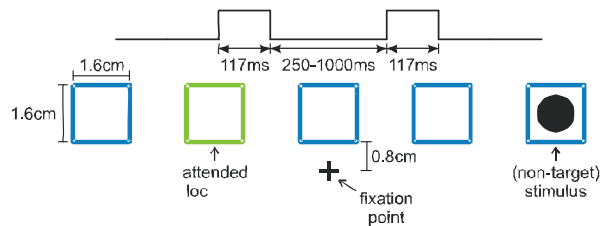
Fig. 1. *View of the task display. Stimulus disks were flashed in five boxes in random order. Subjects responded to stimuli presented in the attended box by a button press.*

Methods

EEG recordings were obtained from twenty-three volunteer subjects ranging in age from 16 to 80 years during performance of a visual selective attention task. Participating subjects, fourteen males and nine females, were right-handed with normal or corrected to normal vision. During 76-second trial blocks, subjects were instructed to attend to one of five squares continuously displayed on a back background 0.8 cm above a centrally located fixation point (Fig. 1). The squares, measuring 1.6 cm by 1.6 cm, were positioned horizontally at angles of 0°, ±2.7° and ±5.5° in the visual field from the point of fixation. Four squares were outlined in blue while one, marking the attended location, was outlined in green (Fig. 1). The location of the attended location was counterbalanced across trial blocks.

Filled white disks were presented for 117 ms within one of the five squares at equally probable inter-stimulus intervals of 250 ms, 500 ms, 750 ms and 1000 ms. During task performance, subjects were required to maintain fixation on the central cross while responding as quickly as possible with a right thumb button press whenever a disk appeared in the attended square. Each subject participated in thirty continuous trial blocks involving presentation of a total of 120 target and 480 non-target stimuli at each of the five locations (Makeig et al., 1999a).

EEG Data. From electrodes mounted in a standard electrode cap, EEG data were recorded at 29 scalp locations in an arrangement adapted from International 10-20 System. Activity produced primarily by eye movements and blinks (plus EEG activity) was obtained from sensors positioned at the left outer canthus and below the right eye. All channels were referenced to the right mastoid. All data was sampled (or in some cases digitally down sampled) at 256 Hz within an analog pass band of 0.1-100 Hz to minimize computational demands during analysis. The experiments were conducted in an electromagnetically unshielded room in which corruptive 60-Hz activity was induced by a nearby commercial (pizza) oven. To eliminate this unwanted activity, appropriate analog (60-Hz notch) and digital (50-Hz low pass) filters were applied during data collection and preprocessing.

Moving-window ICA. Unlike principal component analysis (PCA), ICA attempts to split components with different scalp distributions if their activations (activity time courses) differ. For example, electromyographic (EMG) activity waveforms from different facial and temporal muscles tend to be independent of one another, hence, their spatially distinct and time-course independent EEG activities are decomposed by infomax

into separate components (Jung et al., 1999). An unknown but relatively large number of EEG and artifactual processes may contribute to the human EEG. Infomax ICA, on the other hand, is able to separate at most a number of components equal to the number of recording channels. As input data size is increased, infomax decomposition of ERP recordings may become increasingly more sensitive to over-completeness (i.e., the presence of more active sources than recording channels). Since the activities of most contributing EEG generators may be sparsely distributed across different parts of each trial, separate decompositions of shorter trial sub-epochs may reveal activities that would not be separated by whole-epoch decomposition.

Infomax ICA (Bell & Sejnowski, 1996) may be applied to data samples from concatenated single event-locked time sub-epochs from a collection of single-trial response epochs. One advantage of this approach is the ability to look for the stability of independent components across the event-related epoch. Another purpose was to look for spatially labile components. Since if the time span of a sub-epoch were sufficiently short, the displacement of possible moving sources might be assumed to be negligible within its duration.
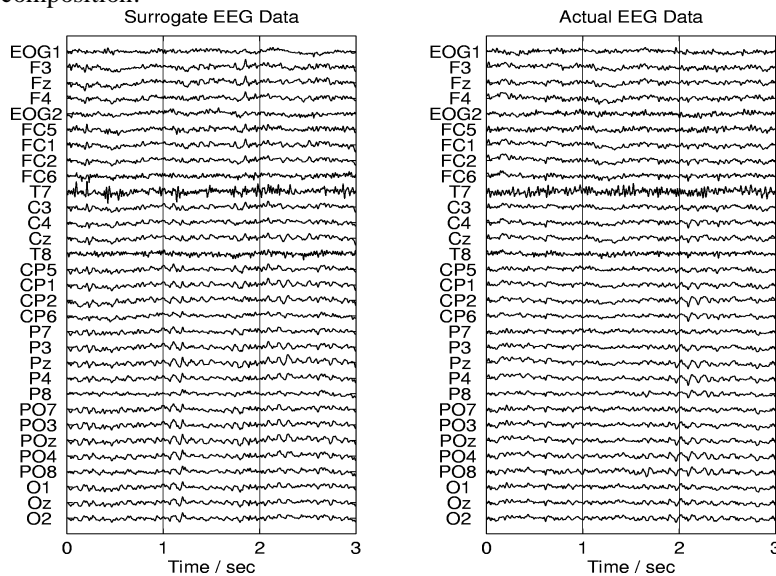
Target Response Decomposition. Moving-window decompositions of 500-600 3-sec EEG epochs (from 1000 ms before to 2000 ms after target stimulus onsets) from each of the 23 subjects were performed on data from each epoch within overlapping 500-ms (128-point) windows successively offset by 5 samples (~20 ms), yielding 129 overlapping sub-epochs. Default *runica()* training parameters were used (Makeig et al., 1998).

Surrogate Data Decomposition. To determine the performance that might be expected from moving-window infomax applied to real EEG recordings, a surrogate EEG data set was constructed to share several properties of the actual EEG data. Two 31-component decompositions of 500-600 ERP target response trials from two subjects constituted the foundation of the surrogate data set. A total of 43 topographically distinguishable components were selected from this 62-component collection. The power spectral density (PSD) of each component's activity was computed using Welch's averaged-periodogram method. From the estimated spectrum, an FIR filter was constructed which, in least-squares terms, matched the component PSD. Amplitude probability distributions functions (PDFs) were also assessed from their respective activity histograms.

Forty-three statistically independent white noise processes with Gaussian distributions and unit variance were generated. Filtering a process with any of the

previously designed EEG component filters caused the PSD of resulting process to match the PSD of the EEG component corresponding to the applied filter. Matching the generally sparse EEG PDFs required transformation of the surrogate process PDFs. These were constructed from the EEG-component and surrogate-process histograms using the MATLAB *histfit()* function. The nonlinear re-mapping of sample values altered the fitted process PSD by reducing attenuation of small activity above 60 Hz. However, as nearly all recorded neural activity of interest occurred in low-frequency bands, the effect of histogram fitting was not noticeable (Fig. 2).

Linear mixtures for each EEG channel were produced by back projection to the scalp and EOG channels via the corresponding EEG-component scalp maps. Component amplitudes were exponentially scaled so as to match the best-fitting exponential fall-off of root-mean square (RMS) amplitude from the largest (1st) to smallest (31st) actual independence component projections from the two subjects. Amplitudes of the 32nd through 43rd surrogate sources were determined by extrapolation of the same exponential. In this manner, 434 surrogate 768-sample data epochs were produced to simulate the original 3-s data epochs on which the surrogate data set was based. Fig. 2 shows selected actual and surrogate data epochs. The surrogate data epochs were then decomposed by ICA using methods identical to those used for target-response decomposition.

sub-epochs had to be identified. Component scalp maps from adjacent sub-epochs were examined to determine which components they shared in common. Map resemblance was defined by a variation of the cross-correlation coefficient in which scalp sensors were considered observations and maps were regarded as variables. A symmetric version of the Mahalanobis distance measure was used for this purpose (Enghoff, 1999).

The maps in a cluster were characterized by the mean cluster map and time course. Matching produced virtual paths through decompositions in successive time sub-epochs, allowing analysis of component map trajectories. Components appearing only in a single decomposition were considered outliers. An intuitive method for visualizing evolving changes in the decompositions was to generate MPEG movies of the sequences of maximally matching maps. The total correlation between the optimally paired maps from successive overlapping sub-epochs was used as a measure of map stability.
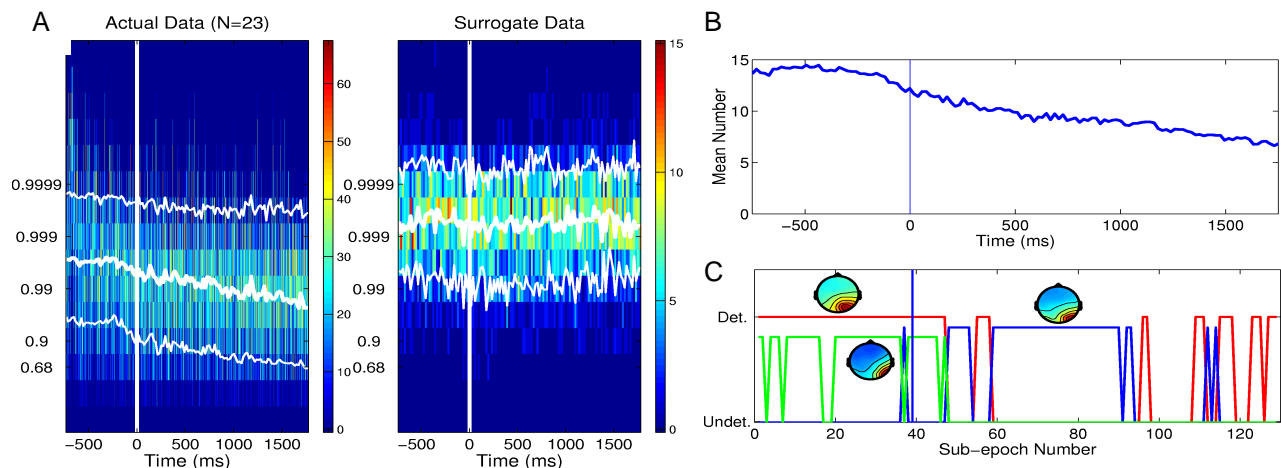
Results

By correlating the original source maps with the merged component maps, on average 19 of the original 43 spatial sources were recovered from the 43-source overcomplete surrogate data set with absolute map correlations above

Fig. 2. Surrogate EEG data set (left) based on the ICA decomposition of the actual EEG data from the subject whose data are shown on the right. Surrogate data were composed by mixing white noise sources whose amplitudes, topographic projections to the scalp, power spectra and probability distributions were filtered to resemble those of the actual subject ICA components. Additional components from another subject were added to the surrogate data to simulate overcompleteness (see text).

Matching Successive Components. Weight matrices resulting from moving-window decomposition were transformed into scalp activity maps by matrix inversion and were then normalized to unity norm. To analyze the evolution of the moving-window components across sub-epochs, matching components in adjacent overlapping

0.85. In many though not all cases, the strongest embedded sources were most accurately recovered. Movies of merged and matched components of the overcomplete surrogate data and of the actual target response data from the subject whose component maps were used as templates for the largest surrogate data

components can be downloaded in full from http://www.cnl.salk.edu/~scott/mapmovies.html. Since the surrogate data movie contains many fewer moving-window-component disappearances and sudden shifts than movies of the actual subject data decompositions, we undertook a closer analysis of component stability in the target-response decompositions.

Map Stability Across Sub-epochs. Fig. 3A (*left panel*) shows histograms of the correlations between the best-paired maps for each pair of adjacent sub-epochs for all 23 subjects. The adjacent-pair correlation histogram for the overcomplete surrogate data set is shown in the right panel. Two facts are evident from Fig. 3A. First, the moving-window ICA decompositions of the actual target response data became clearly less stable after stimulus presentation. For example, the 10th percentile of correlation in the final sub-epoch (*left panel, lower trace, right side*) was 0.674, while the 10th percentile of the surrogate data correlations never dipped below 0.974.

patterns in single trials (Jung et al., in press). Consistent with the sub-epoch correlation results, the mean number of components per sub-epoch decomposition contributing to the 40 moving-window component clusters declined from 14 before stimulus onset to 7 at the end of the epoch (Fig. 3B). Although the sub-epoch decompositions contained several components (typically, among the smallest) with noiselike or 'blotchy' maps, none of the 40 cluster maps contained more than one (monopolar) or two (bipolar) spatial maxima.

Fig. 3C (below) shows a case in which three moving-window component clusters from one subject were included in a single between-subjects cluster. Two of these were separated out concurrently from sub-epochs in the pre-stimulus period. However, in sub-epochs centered 175 ms or more following stimulus onset, the two components were replaced with a single similar component.

Fig. 3. *(A) Histograms of the correlations between best-matched component pairs in adjacent overlapping sub-epochs for the surrogate data set (right) and the actual EEG data (mean of 23 Ss). White lines show the 10th, 50th and 90th percentiles of the distributions. (B) The number of sub-epoch components clustered, indexed by the center time of the sub-epoch window (23 Ss). (C) Sub-epochs in which 3 moving-window component clusters were detected (1 S).*

Second, even in the pre-stimulus period the decompositions of the actual data were somewhat less stable than the surrogate decompositions.

Between-Subjects Component Similarity. For each subject, all 31x129 (stimulus-locked) maps from the moving-window decompositions were clustered without regard to time of occurrence, yielding 80 component clusters (or "moving-window components") per subject. Mean scalp maps for these 1840 (80x23) moving-window components were then clustered, again without regard for their times of occurrence. Of the resulting 40 "between-subjects" clusters, several accounted for eye blinks, lateral eye movements or temporal muscle activity, as judged by their scalp maps, mean spectra and activity

Component Mobility. Examination of the MPEG movies of the merged moving-window components revealed little or no evidence of independent components moving fluidly across the scalp. Instead, the observed spatial instability in the moving-window components was comprised mainly of (1) abrupt jumps (when a moving-window component was no longer detected and a distinctly different component was assigned its place in the map array), and (2) fluctuations in the peripheral extent but not the focus of the active scalp region.

Equivalent-dipole source modeling was performed on three such moving-window components from the central posterior alpha cluster using a three-shell spherical model (Scherg & Ebersole, 1994). These component series

could be well fit by two opposing equivalent current dipoles located approximately in the left and right banks of the central fissure in the occipital lobe near the calcarine sulci. In two of the subjects, this posterior alpha moving-window component composed of maps from all sub-epochs. In the third, a similar component was detected in sub-epochs centered before 245 ms after stimulus onset. In all three subjects, the variability in the scalp map throughout the detection period could be well modeled by changes in the relative strengths (but not the locations) of the two dipoles. The residual variance of the two-dipole models to the entire observed sequences of component maps were low (< 5%).

Oscillatory Component Clusters. At least four other clusters accounted for posterior alpha moving-window components (each drawing from 6-12 subjects). These clusters included a preponderance of pre-stimulus sub-epochs. Altogether, 18 of the 23 subjects contributed one or more components to these four clusters. Another subject contributed a component to the central occipital alpha cluster. The alpha peak in all four component spectra was at 10 Hz. All four between-subjects mean cluster maps could be fit by single equivalent dipoles located in left or right occipital cortex with very low residual variance ($1.25\% \pm 0.8\%$).

Three or more between-subjects component clusters accounted for centrolateral mu activity, circa 10-Hz rhythms of the motor cortex with a second spectral peak near 20 Hz, sometimes giving them their prototypical 'μ' shape. Moving-window component maps belonging to these clusters came from 20 of the 23 subjects, but not from sub-epochs following the button press, in which mu activity was blocked (Makeig et al., in press). Sequences of maps forming moving-window mu components could also be accounted for by single equivalent dipole models with low (<5%) residual variance. Moreover, these models placed the equivalent dipole close to the known location of the hand motor areas in the middle of the left and right central sulci.

Moving-window versus Whole-epoch Decomposition. To determine the stability and completeness of the moving-window decompositions relative to decomposition of the whole epochs, each subject's 3-s target-response trials were decomposed in a single ("whole-epoch") decomposition, yielding 31 independent components. Following decomposition, the 713 (31x23) whole-epoch components from all subjects were clustered in the same manner as the moving-window components. The mean maps for the resulting 80 whole-epoch component clusters were then correlated with the mean maps of the 80 between-subjects moving-window component clusters.

Altogether, 23 between-subjects component pairs were correlated above 0.90. Some of these clearly accounted for artifacts (eye movements, temporal muscles). Both decomposition methods also separated similar (map r>0.90) alpha and mu component clusters. However, the number of subjects included in the moving-window component clusters was about 65% larger than the number contributing to the corresponding whole-epoch clusters.

Discussion

Concatenated, the ~500 3-s data epochs from each subject comprised about 25 minutes of EEG data. Performing a single (whole-epoch) decomposition of this much data is not necessarily the best strategy for separating the underlying neural (and artifactual) data sources. Over many minutes, many more brain areas (and/or EEG artifacts) might become coherently active, producing more spatial EEG patterns on the scalp than the number of recording channels. Two possible strategies for overcoming this potential overcompleteness problem: Either make more restrictive assumptions about the components or their activity distributions, allowing the use of overcomplete ICA algorithms (Lewicki & Sejnowski, in press), or else divide the data into shorter training sets. Here we applied the second strategy. Moreover, instead of separating the data into epoch groups from the beginning, middle and end of the test session, we separated the data matrix into overlapping sub-epochs defined by their time relationship to target stimulus presentations. This approach tacitly assumes stationarity of the EEG spatial structure across the session, but allowed us to assess rapid event-related variations in its spatial structure time.

We found several such variations. First, the number of component maps that were clustered with a symmetric Mahalanobis metric was twice as large before target stimulus presentation as at epoch end two seconds later. Several categories of components participated in this trend, notably posterior alpha and central mu components, whose moving-window component maps were sufficiently similar in large numbers of subjects to be grouped into between-subject clusters by the same algorithm. Components accounting for eye and muscle activity, however, tended to be active throughout the epoch.

There may be multiple reasons why fewer alpha and mu components were separated by moving-window decomposition of sub-epochs following stimulus onset. Characteristic mu component activity near 10 Hz and 20 Hz was blocked following the button press (Makeig et al., in press). The amplitude of posterior alpha activity, meanwhile, was hardly if at all affected by stimulus

presentation. Typically, however, we have found that following visual stimulus presentation the phase of alpha components may be reset to a common value. Resetting the phase of two or more alpha components concurrently might thereby collapse their independence, reducing the number of such components separated in later sub-epoch decompositions. Whether or not these explanations together account for the preponderance of alpha-band and other (e.g., frontal) components in the pre-stimulus epoch clusters is a subject for further research.

Another important fact emerging from the two-stage clustering procedure was that complex, blotchy or noisy-appearing maps, although found in every decomposition, were never clustered between subjects and rarely between sub-epochs, thereby suggesting they represented unresolved mixtures of low-level sources and/or noise. Exceptions to this rule were the cluster of stable and simple-appearing central occipital alpha components found in six of the subjects. Source modeling of these components required two coherently active current dipoles located in the left and right occipital pole. However, other common alpha component maps could be very well accounted for by single dipoles.

This suggests that the basic and important principle of brain *spatial* modularity, which posits that brain processing is carried out in multiple circa-cm^2 brain regions, should be augmented to include a principle of *dynamic* modularity, wherein coherently synchronous activities occurring within different modular brain areas are substantially independent of one another. The relative independence of spike trains in individual even nearby neurons has long been viewed as a basic fact of neuroscience. The relative independence of *coherent* activity in different modular brain areas is suggest by their decomposition by ICA into separate components that can be modeled using a single equivalent source dipole. ICA decomposition (either moving-window or whole-epoch) then allows examination of event-related modulations of the dynamic independence of different brain areas.

While our results suggest the number of brain areas making major contributions to scalp EEG may be relatively few (certainly less than the number of active brain areas), non-invasive examination of dynamics in and between active brain networks appears to afford a real scientific opportunity for system-level modeling of the neural substrates of cognition. The fact of spatial brain modularity, meanwhile, creates the opportunity for spatial ICA to separate important sources of blood oxygen level difference (BOLD) signals recorded in brain functional magnetic resonance imaging (fMRI) experiments (McKeown et al., 1998).

One near term goal of our research is to compare the results presented here with those obtained from ICA decomposition of higher-density EEG (or MEG) recordings. Further research into methods for assessing the dynamics of brain activity within and between independent components may give the field of cognitive neuroscience important new tools for exploring and characterizing systems-level brain dynamics accompanying or underlying human cognition.

References

Bell, A. J., Sejnowski, T. J. *Neural Computation* 7:1129 -1159, 1995.

Enghoff, S *Tech. Report* INC-9902, Institute for Neural Computation, Univ. Calif., La Jolla CA, 1999.

Jung, T. P., Humphries, C. Lee, T.-W., Makeig, S., McKeown, M. J., Iragui, V. and Sejnowski, T. J., *Adv Neural Info Proc Sys*, 10:894-900, 1998.

Jung, T-P., Makeig, S., Westerfield, M., Townsend, J., Courchesne, E., Sejnowski, T. J. *Adv Neural Info Proc Sys 11*. pp. 894-900. Cambridge, MA: MIT Press, 1999.

Jung T-P, Humphries C , Lee TW, McKeown MJ, Iragui V, Makeig S, Sejnowski TJ, *Psychophysiolog*, in press.

Lewicki, M., Sejnowski, T. J., *Neural Comput*, in press.

McKeown, M. J., Makeig, S., Brown, G. G., Jung, T-P., Kindermann, S. S., Bell, A. J., Sejnowski, T. J. *Human Brain Mapping* 6:160-188, 1998.

Makeig, S., Bell, A. J., Jung, T-P., Sejnowski, T. J. *Adv Neural Info Proc Sys 8* pp. 145-151. Cambridge, MA: MIT Press , 1996.

Makeig, S., Jung, T-P., Ghahremani, D., Bell, A.., Sejnowski, T. J., *Proc Natl Acad Sci USA* 94:10979 10984, 1997.

Makeig, S. *et al. WWW Site*, Computational Neurobiology Laboratory, Salk Institute, La Jolla CA, http://www.cnl.salk.edu/~scott/ica.html, 1998.

Makeig, S., Westerfield, M., Jung, T-P., Covington, J., Townsend, J., Sejnowski, T. J., Courchesne, E., *J Neurosci* 19:2665 2680, 1999a.

Makeig, S., Westerfield, M., Townsend, J., Jung, T.-P., Courchesne, E., Sejnowski, T. J., *Phil Trans: Biol Sci, The Royal Society* 354:1135-44, 1999b.

Makeig, S., Enghoff, S., Jung, T.-P., Sejnowski, T. J., *IEEE Trans Rehab Eng,* in press.

Scherg M, Ebersole JS. *Brain Topogr* 5:419-23, 1993.

Vigario RN, *Electroencephalogr Clin Neurophysiol* 103:395-404, 1997.